

Synthesis and crystal structure of the feldspathoid CsAlSiO₄: An open-framework silicate and potential nuclear waste disposal phase

G. DIEGO GATTA,^{1,2,*} N. ROTIROTI,^{1,2} P.F. ZANAZZI,³ M. RIEDER,⁴ M. DRABEK,⁵ Z. WEISS,^{4,†}
AND R. KLASKA⁶

¹Dipartimento di Scienze della Terra, Università degli Studi di Milano, Italy

²CNR-Istituto per la Dinamica dei Processi Ambientali, Milano, Italy

³Dipartimento di Scienze della Terra, Università degli Studi di Perugia, Italy

⁴Institute of Materials Chemistry, VSB, Technical University of Ostrava, Czech Republic

⁵Czech Geological Survey, Prague, Czech Republic

⁶HeidelbergCement AG, Ennigerloh, Germany

ABSTRACT

Crystalline CsAlSiO₄ was synthesized from a stoichiometric mixture of Al₂O₃ + SiO₂ + Cs₂O (plus excess water) in Ag-capsules at hydrostatic pressure of 0.1 GPa and temperature of 695 °C. The duration of synthesis was 46 h. The crystal structure of CsAlSiO₄ was investigated by single-crystal X-ray diffraction. The structure is orthorhombic with *Pc2₁n* space group and lattice parameters: *a* = 9.414(1), *b* = 5.435(1), and *c* = 8.875(1) Å. Because of the orthohexagonal relation between *b* and *a* (*a* ≈ *b*√3), within the standard uncertainty on the lattice parameters, a hexagonal superlattice exists, which is responsible for twinning. The crystals are twinned by reflection, with twin planes (110) and (310): twinning in both cases is by reticular merohedry with twin index 2 and hexagonal twin lattice (*L_T*). The transformation from the lattice of the individual (*L_{ind}*) to *L_T* is given by: *a_T* = *a_{ind}* – *b_{ind}*, *b_T* = 2*b_{ind}*, and *c_T* = *c_{ind}*. The refinement was initiated using the previously published atomic coordinates for RbAlSiO₄. The final least-square cycles were conducted with anisotropic displacement parameters. *R*₁ = 3.04% for 66 parameters and 2531 unique reflections. For a more reliable crystallographic comparison the crystal structure of RbAlSiO₄ is reinvestigated here adopting the same data collection and least-squares refinement strategy as for CsAlSiO₄.

The crystal structure of the CsAlSiO₄ feldspathoid is built on an ABW framework type, showing a fully ordered Si/Al-distribution in the tetrahedral framework. The only extra-framework site is occupied by Cs, lying off-center in the 8mR-channels. CsAlSiO₄ is more likely to retain Cs when immersed in a fluid phase, relative to several other Cs-bearing zeolites. The topological configuration of the Cs-polyhedron (and its bonding environment), the small dimension of the pores and the high flexibility of the ABW framework type would imply a better thermal and elastic stability of CsAlSiO₄ than those of the zeolitic Cs-aluminosilicates. In this light, CsAlSiO₄ can be considered as a functional material potentially usable for fixation and deposition of radioactive isotopes of Cs and can also be considered as a potential solid host for a ¹³⁷Cs γ-radiation source to be used in sterilization applications.

Keywords: CsAlSiO₄, RbAlSiO₄, ABW framework type, feldspathoid, crystal structure, nuclear waste disposal phase

INTRODUCTION

Cesium-bearing minerals are rare, most often found in pegmatite minerals, e.g., Cs-rich beryl and pezzottaite [Cs(Be₂Li)Al₂Si₆O₁₈, Hawthorne et al. 2004]. In rock-forming silicates, Cs can partially replace K in framework silicates or phyllosilicates such as Cs-biotite (Hess and Fahey 1932) or nanpingite (Ni and Hughes 1996). Only a few structures of natural and synthetic Cs-aluminosilicates are known, such as pollucite (CsAlSi₂O₆, Newnham 1967; Beger 1969), the Cs-4A zeolite (Vance and

Seff 1975; Firor and Seff 1977) and Cs-bikitaite (CsAlSi₃O₁₂, Araki 1980). All of them form open-framework structures like feldspathoids or zeolites. Cesium aluminosilicate, CsAlSiO₄, grew in several hydrothermal experiments aimed at the synthesis of a muscovite-type cesium mica, a suitable crystalline phase potentially usable as nuclear waste disposal material (Mellini et al. 1996; Drábek et al. 1998; Comodi et al. 1999).

There has been no determination of the structure of CsAlSiO₄ in the open literature. Synthesis, optical properties, and crystal-structure of CsAlSiO₄ were first studied by Klaska (1977), in his doctoral dissertation. However, the structural data were not published and, as a consequence, they are not at present available in any crystallographic database. At the same time, but

* E-mail: diego.gatta@unimi.it

† Deceased May 3, 2005.

independently, Gallagher et al. (1977) synthesized CsAlSiO₄ from cesium oxide, alumina, and silica under different firing conditions. Based on the structural data of RbAlSiO₄ (Klaska and Jarchow 1975), Gallagher et al. (1977) indexed the X-ray powder diffraction pattern of CsAlSiO₄ on an orthorhombic unit cell with $a = 8.907(2)$, $b = 9.435(1)$, and $c = 5.435(1)$ Å and $Pna2_1$ space group. However, no structural refinement was performed. Accordingly, the crystal structure of CsAlSiO₄ is expected to show strong analogies with that of RbAlSiO₄.

The crystal structure of RbAlSiO₄ was solved by Klaska and Jarchow (1975) in the $Pc2_1n$ space group with lattice parameters $a = 9.22(6)$, $b = 5.33(7)$ and $c = 8.74(1)$ Å, by means of single-crystal X-ray diffraction. The authors found the diffraction pattern to be metrically hexagonal, but they had to treat it as due to a triple twin of orthorhombic individuals, with twinning planes (110) and (130) (in the reciprocal space, Fig. 3 in Klaska and Jarchow 1975), simulating hexagonal symmetry (Fig. 1). The crystal structure of RbAlSiO₄ is built on an ABW framework type (Baur and Fischer 2000; Baerlocher et al. 2001), shown in Fig. 2. This framework type consists of tetrahedral sheets parallel to (001), in which six-membered rings (6mRs) of corner-sharing tetrahedra define channels parallel to [001] (in the $Pc2_1n$ setting, Fig. 3). Apical O atoms of three neighboring tetrahedra in a ring point upward, whereas apical O atoms of the other three tetrahedra point down (Figs. 3 and 4). Channels consisting of distorted eight-membered ring (8mRs) channels run along [010] where the extra-framework sites lie (Fig. 4). The cell parameters of an idealized ABW structure (i.e., a hypothetical Si_nO_{2n} framework structure obtained by performing a distance least-squares (DLS) refinement in the topological space group, Baerlocher et al. 2001) are $a = 9.873$, $b = 5.254$, and $c = 8.770$ Å, with $Imma$ space group and a framework density $FD_{Si} = 17.6$ T/1000 Å. As shown later by Klaska (1977), CsAlSiO₄ and RbAlSiO₄ are two isotopic open-framework silicates with same general symmetry (space group $Pc2_1n$), similar lattice parameters [$a = 9.44(3)$, $b = 5.43(5)$, and $c = 8.89(2)$ Å for CsAlSiO₄] and because of the

orthohexagonal relation between b and a ($a \approx b\sqrt{3}$) they show the same twinning by reticular merohedry, as described above. About 100 compounds with ABW topology are known as reviewed by Baur and Fischer (2000) and Kahlenberg et al. (2001). Hahn et al. (1969) and Liebau (1985) defined the compounds with an ABW framework as belonging to the “*Icmm*-type” structural family. However, no mineral has yet been found with this framework type.

Among the large number of compounds with ABW topology, the aluminosilicates RbAlSiO₄ and TlAlSiO₄ (and the Cs-aluminotitanate CsAlTiO₄, at least for the Cs-bonding environment) are expected to have strong structural homologies with CsAlSiO₄. Krogh Andersen et al. (1991) reported the crystal structure of TlAlSiO₄ [with $a = 8.297(1)$, $b = 9.417(1)$, $c = 5.413(1)$ Å, space group $Pna2_1$] based on Rietveld refinement of X-ray powder diffraction data, adopting the structural model of RbAlSiO₄. Later, the crystal structure of TlAlSiO₄ was reinvestigated by Kyono et al. (2000) by single-crystal X-ray diffraction. The authors described the structure as monoclinic with $P2_1/n$ space group and $a = 5.4095(3)$, $b = 9.4232(7)$, $c = 8.2629(6)$ Å, and $\gamma = 90.01(2)^\circ$. The structural models of TlAlSiO₄ reported by Krogh Andersen et al. (1991) and Kyono et al. (2000) are basically consistent with a fully ordered distribution of Si and Al in the tetrahedral framework. The lowering of symmetry from orthorhombic to monoclinic as reported by Kyono et al. (2000) appears to be caused by the inert-pair effect of the Tl⁺ cation. The authors did not report any evidence of twinning for the TlAlSiO₄ crystals as previously observed for RbAlSiO₄ and CsAlSiO₄ by Klaska and Jarchow (1975) and Klaska (1977), respectively. The crystal structure of CsAlTiO₄ was solved by Gatehouse (1989) from single-crystal X-ray diffraction data with $a = 8.978(4)$, $b = 5.740(1)$, and $c = 9.969(2)$ Å and $Imma$ space group. The Al/Ti distribution in the tetrahedral framework was found to be completely disordered, thus making the symmetry higher relative to RbAlSiO₄ and TlAlSiO₄. The aforementioned compounds (i.e., RbAlSiO₄, CsAlSiO₄, TlAlSiO₄, and CsAlTiO₄) show how the

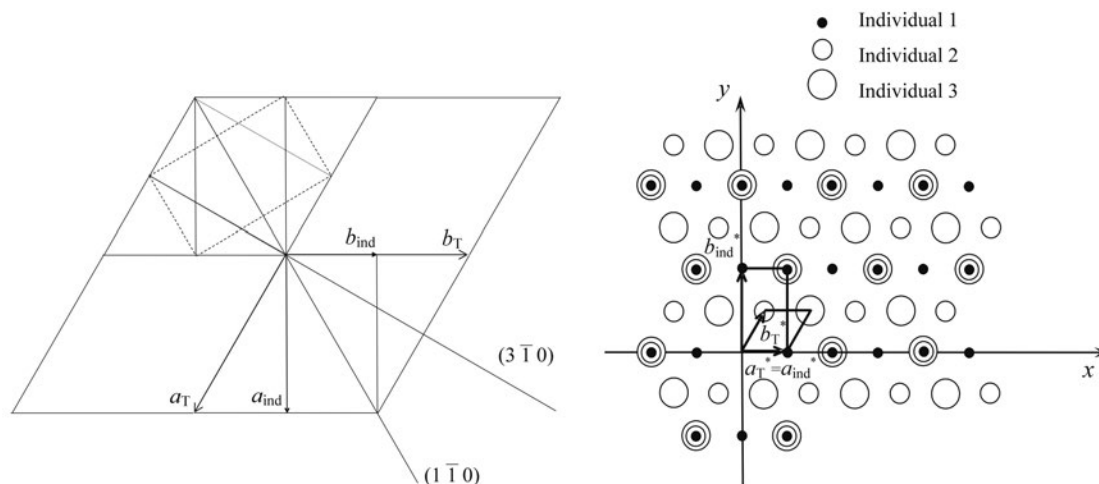


FIGURE 1. (left side) Geometrical relationship between the (hexagonal) twin lattice (T) and that of the orthorhombic individuals (ind) of CsAlSiO₄ represented in the direct space, where $\mathbf{a}_T = \mathbf{a}_{ind} - \mathbf{b}_{ind}$, $\mathbf{b}_T = 2\mathbf{b}_{ind}$ and $\mathbf{c}_T = \mathbf{c}_{ind}$, and (right side) reconstruction of the diffraction pattern in the reciprocal space. The crystals are twinned by reflection, with twin planes (110) and (310). Twinning is by reticular merohedry.

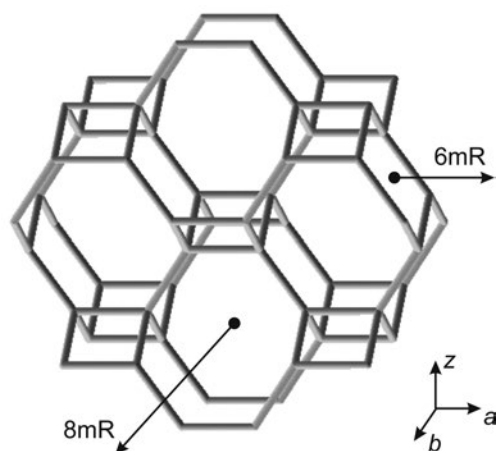


FIGURE 2. Skeletal representation of the idealized ABW framework type described with *Imma* symmetry.

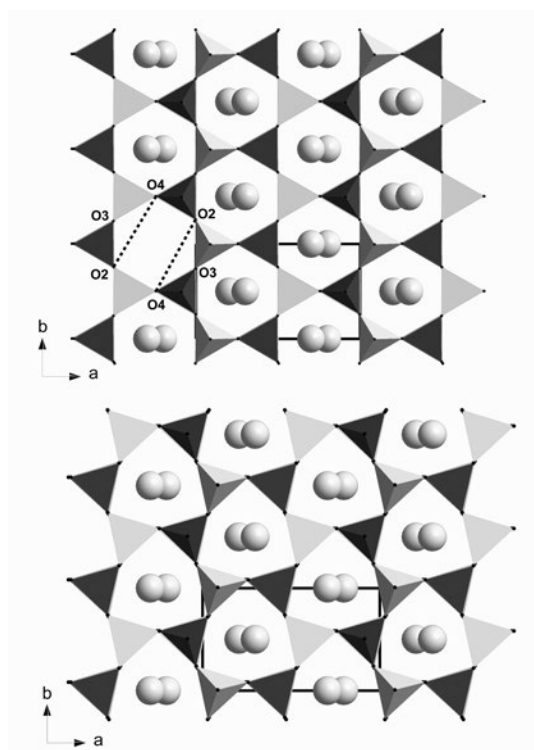


FIGURE 3. The crystal structure of (above) CsAlSiO₄ and (below) RbAlSiO₄ viewed down [001], based on the data of this study. Dark-gray tetrahedra represent the Si-tetrahedra, whereas light-gray tetrahedra represent the Al-occupied ones. Large spheres represent the Cs or Rb sites.

general symmetry among this class of materials can be different, despite the same framework topology.

The aim of this study is the crystal-structure re-investigation of CsAlSiO₄, making the structural data of this compound available in the open literature. In addition, we describe the structural homologies with other isotopic compounds, in particular RbAlSiO₄, TlAlSiO₄, and CsAlTiO₄, and non-isotypic compounds of mineralogical interests, with a framework containing six-

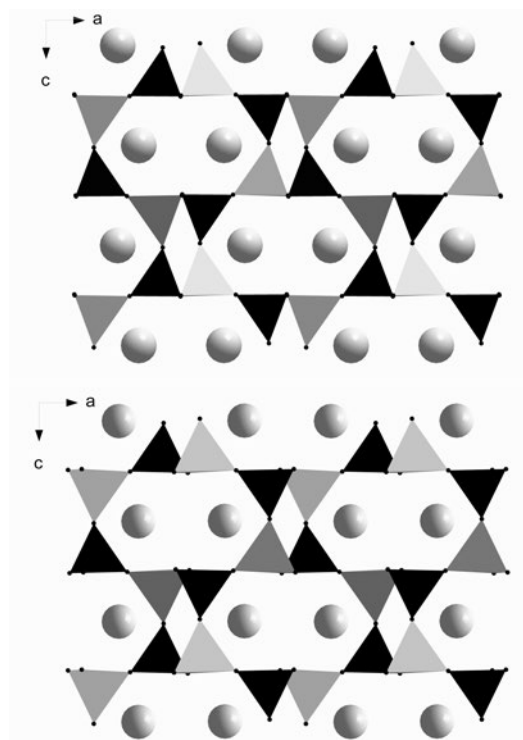


FIGURE 4. The crystal structure of (above) CsAlSiO₄ and (below) RbAlSiO₄ viewed down [010], based on the data of this study. Dark-gray tetrahedra represent the Si-tetrahedra, whereas light-gray tetrahedra represent the Al-occupied ones. Large spheres represent the Cs or Rb sites.

membered rings as building block units (i.e., stuffed-tridymite structures, like nepheline and kalsilite). For a more reliable crystallographic comparison, the crystal structure of RbAlSiO₄ was reinvestigated adopting the same data collection and least-square refinement strategy as for CsAlSiO₄.

EXPERIMENTAL METHODS

The presently investigated sample of CsAlSiO₄ was synthesized in run no. Cs-116 from a stoichiometric proportion of Al₂O₃ + SiO₂ + Cs₂O (plus excess water) in Ag-capsules at hydrostatic pressure of 0.1 GPa and temperature of 695 °C. The duration of the experiment was 46 h. The crystals of RbAlSiO₄ were grown by A. E. Beswick, at the Johns Hopkins University, Baltimore, in experiments aimed at determining the K/Rb distribution between sanidine and vapor. The experiments were conducted at 0.2 GPa and temperatures of 500, 700, and 800 °C. The RbAlSiO₄ phase grew in Rb-rich charges. It was referred to as the "orthorhombic phase" (Beswick 1973).

Electron microprobe analysis of the same sample of CsAlSiO₄ used for the X-ray diffraction experiment was performed using a fully automated CAMECA SX-50 microprobe operating in WDS mode. Major and minor elements were determined at 15 kV accelerating voltage and 10 nA beam current with a counting time of 20 s. Pollucite was used as the standard for Cs, Al, and Si. The crystal was found to be homogeneous within analytical error. The composition agrees with the ideal chemical formula within the estimated standard deviation: Cs_{0.99(2)}Al_{0.99(2)}Si_{1.01(3)}O₄.

Two crystals of CsAlSiO₄ and RbAlSiO₄, free of defects on the optical scale, were selected for the X-ray diffraction experiments. X-ray single-crystal diffraction data of CsAlSiO₄ and RbAlSiO₄ were collected at room conditions with an Oxford Diffraction-Xcalibur diffractometer equipped with CCD, using a graphite monochromator for MoK α -radiation, operated at 50 kV and 30 mA. To maximize the reciprocal space coverage, a combination of ω and ϕ scans were used, with a step size of 0.5° and a time of 25 s/frame (Table 1). The distance between the

crystal and the detector was 60.4 mm

For CsAlSiO₄, 3945 "observed" reflections [with $I > 3\sigma(I)$] in the range $3 < 2\theta < 62^\circ$ were collected (Table 1) giving metrically hexagonal cell parameters: $a = b = 10.870(1)$ Å, $c = 8.875(1)$ Å. After Lorentz, polarization, and analytical absorption corrections using the CrysAlis package (by Gaussian integration based upon the physical description of the crystal, Oxford Diffraction 2005), the discrepancy factor among symmetry related reflections was $R_{\text{int}} \approx 42\%$. A similar R_{int} value was also obtained without any absorption correction to the diffraction data. On the basis of Klaska and Jarchow's (1975) experience with RbAlSiO₄, we treated the diffraction pattern as due to orthorhombic individuals, with $a = 9.414(1)$, $b = 5.435(1)$, and $c = 8.875(1)$ Å (Table 1), twinned by reflection with twin planes (110) and (310). Twinning is by reticular merohedry, with twin index 2 and the hexagonal twin lattice (L_T) (see above) (Fig. 1). The transformation from the lattice of the individual (L_{ind}) to L_T is given by: $\mathbf{a}_T = \mathbf{a}_{\text{ind}} - \mathbf{b}_{\text{ind}}$, $\mathbf{b}_T = 2\mathbf{b}_{\text{ind}}$ and $\mathbf{c}_T = \mathbf{c}_{\text{ind}}$. On the basis of the reflection conditions ($0kl$ with $l = 2n$; hkl with $h + k = 2n$), the assigned space group is $Pc2_1n$, according to Klaska and Jarchow (1975) and Klaska's (1977) findings for RbAlSiO₄ and CsAlSiO₄, respectively. As shown in Figure 1, several classes of reflections belonging to the three orthorhombic individuals are fully overlapped.

Similar data collection strategy was adopted for RbAlSiO₄. In this case, 3277 "observed" reflections in the range $3 < 2\theta < 62^\circ$ were collected, giving a metrically hexagonal diffraction pattern due to threefold twinning of orthorhombic individuals with cell parameters: $a = 9.217(1)$, $b = 5.321(1)$, and $c = 8.724(1)$ Å (Table 1). The integrated intensity data were corrected for Lorentz-polarization and absorption effects and used for structural refinement.

Structural refinements of CsAlSiO₄ and RbAlSiO₄

The structural refinements of CsAlSiO₄ and RbAlSiO₄ were carried out using JANA2000 package (Petříček and Dušek 2000), using the implemented special routine for 3-individuals twinning. For CsAlSiO₄, the average R_{int} value was 0.1013 (Table 1). The refinement was conducted starting from the atomic coordinates of Klaska and Jarchow (1975) (substituting Rb with Cs) with isotropic displacement parameters in the space group $Pc2_1n$ using neutral atomic scattering factor values. A structure refinement performed using the ionic scattering curves did not provide significantly different results. The final least-square cycles were conducted with anisotropic displacement parameters. When convergence was achieved, the final agreement index (R_1) was 0.0304 for 66 refined parameters and 2560 unique reflections.

TABLE 1. Details pertaining to the data collection and refinement of CsAlSiO₄ and RbAlSiO₄

	CsAlSiO ₄	RbAlSiO ₄
Crystal size (mm ³)	0.20 × 0.12 × 0.06	0.18 × 0.14 × 0.08
Diffractometer	Xcalibur CCD	Xcalibur CCD
X-ray radiation	MoK α	MoK α
Scan type	ω/ϕ	ω/ϕ
Scan width ($^\circ$ /frame)	0.5	0.5
CCD frames processed	1402	1402
Exposure (s/frame)	25	25
Temperature	293 K	293 K
Space group	$Pc2_1n$	$Pc2_1n$
Cell dimensions (Å)	$a = 9.414(1)$ $b = 5.435(1)$ $c = 8.875(1)$	$a = 9.217(1)$ $b = 5.321(1)$ $c = 8.724(1)$
Z	4	4
ρ_{calc} (g/cm ³)	3.685	3.174
Extinction coefficient, g_{iso} *	0.09532	0.0364
Maximum 2θ	62°	62°
Index range	$-13 \leq h \leq 13$ $-7 \leq k \leq 7$ $-12 \leq l \leq 12$	$-13 \leq h \leq 13$ $-7 \leq k \leq 7$ $-12 \leq l \leq 12$
Measured reflections	8215	8474
Observed reflections [with $I > 3\sigma(I)$]	3945	3277
Unique reflections (over all the individuals)	2560	2199
R_{int}	0.1013	0.1306
Number of l.s. parameters	66	66
$R_1, F_o > 3\sigma(F_o)$	0.0304	0.0538
R_1 , all data	0.0618	0.1252
wR_2 (on F_o^2)	0.0710	0.1019
Refined volume of each individual	$V_1 \approx 15\%$ $V_2 \approx 2\%$ $V_3 \approx 83\%$	$V_1 \approx 7\%$ $V_2 \approx 6\%$ $V_3 \approx 87\%$

Note: R_{int} is calculated on the basis of all the measured reflections.

* As implemented in JANA2000.

tions (overall the three individuals) with $F_o > 3\sigma(F_o)$. Further details pertaining to the refinement are reported in Table 1. At the end of the last refinement cycle, no peaks larger than $\pm 0.88 \text{ e}^-/\text{\AA}^3$ were present in the final difference-Fourier map. Positional and displacement parameters are reported in Table 2. Relevant bond lengths and geometrical parameters are listed in Table 3. Observed and calculated structure factors (for all the three individuals) are reported in Table 4¹. A further structural refinement was conducted in the centrosymmetric space group $Pcmm$. However, the refinement led to a slightly worse final agreement index (R_1) than that in the non-centrosymmetric space group $Pc2_1n$.

To prove that the symmetry of CsAlSiO₄ is indeed orthorhombic, as for RbAlSiO₄, and not monoclinic, as for TlAlSiO₄, a further structural refinement was performed in the monoclinic space group $P2_1/n$ (with $\beta = 90^\circ$) adopting the atomic coordinates reported by Kyono et al. (2000), transformed to the b -unique setting. The refinement was conducted adopting the same strategy as described for the refinement in orthorhombic symmetry. We compared the results of the orthorhombic and monoclinic refinements on the basis of two criteria: (1) same number of reflections within the same resolution limit, and (2) equal ΔF cut-off ($\Delta F = F_{\text{obs}} - F_{\text{calc}}$). Following the first criterion, we observed (1) some Si-O distances were longer than 1.7 Å; (2) some Al-O distances were shorter than 1.6 Å; (3) several T-O-T and O-T-O bond angles gave anomalous values; (4) complete convergence was not fully achieved (with a residual value of the change/standard uncertainty); and (5) the residual peaks in the final difference-Fourier map were $\rho_{\text{max}} = +4.3 \text{ e}^-/\text{\AA}^3$ and $\rho_{\text{min}} = -3.0 \text{ e}^-/\text{\AA}^3$. Following the second criterion, we observed that the refinement converged, but (1) the Si/Al-tetrahedra appeared to be less regular than those in the orthorhombic symmetry; (2) the agreement parameters ($R_{\text{int}}, R_1, wR_2$) were slightly worse with respect to those obtained in the orthorhombic refinement; and (3) the residual peaks in the final difference-Fourier map were $\rho = \pm 1.1 \text{ e}^-/\text{\AA}^3$. From this, we conclude that the symmetry of CsAlSiO₄ is truly orthorhombic, with $Pc2_1n$ space group.

Polycrystalline CsAlSiO₄ was grown in another experiment (no. Cs-49) from a stoichiometric proportion of kaolinite "Bohemia" + Cs₂O (plus excess water) at 0.1 GPa and temperature 413–430 °C, duration 191 h. Structure refinement of this phase was performed on graphite-monochromatized CoK α radiation powder data using the GSAS program (Larson and Von Dreele 2000). After correction for microabsorption (Pitschke et al. 1993), the refinement was performed in both monoclinic and orthorhombic settings. Both converged to about the same R_1 of 0.065 and, within the precision of the resulting coordinates, no significant difference between the two models was observed. However, the essential features of the structure were essentially the same as those from the single-crystal refinement: the nearly perfect hexagonal rings of tetrahedra, the alternation of Al and Si tetrahedra, and the asymmetric positioning of Cs in the large cavity. The March-Dollase coefficient indicated a mild preferred orientation on (001), parallel to the plane of 6mRs. This indicates the existence of a cleavage or platy morphology of particles in the powder mount. The quality of the Rietveld refinement is inferior in comparison with the single-crystal data, hence we do not present the results here.

For RbAlSiO₄ single-crystal data, the discrepancy factor among symmetry related reflections was $R_{\text{int}} = 0.1306$ (Table 1). The refinement was conducted starting from the atomic coordinates of Klaska and Jarchow (1975) with isotropic displacement parameters in the space group $Pc2_1n$, using neutral atomic scattering factor values. The final least-square cycles were conducted with the anisotropic displacement parameters. The refined displacement ellipsoids of the atomic sites belonging to the tetrahedral framework appear to be strongly anisotropic. Despite the fact that the quality of the diffraction data of RbAlSiO₄ is lower than that for CsAlSiO₄, likely due to the poorer quality of the crystal, the final agreement index (R_1), calculated for 66 refined parameters and 2199 unique reflections (overall the 3 individuals), with $F_o > 3\sigma(F_o)$, was 0.0538 (Table 1). No peaks larger than $\pm 0.98 \text{ e}^-/\text{\AA}^3$ were found in the final difference-Fourier map. However, the variance-covariance matrix of the final refinement cycle showed a significant correlation (~80%) between some of the refined parameters. Further details of the structural refinement are reported in Table 1. Atomic positions and displacement parameters

¹ Deposit item AM-08-030, Table 4 (observed and calculated factors) and CIF. Deposit items are available two ways: For a paper copy contact the Business Office of the Mineralogical Society of America (see inside front cover of recent issue) for price information. For an electronic copy visit the MSA web site at <http://www.minsocam.org>, go to the American Mineralogist Contents, find the table of contents for the specific volume/issue wanted, and then click on the deposit link there.

TABLE 2. Fractional atomic coordinates and displacement parameters (Å²) of (above) CsAlSiO₄ and (below) RbAlSiO₄

Site	x	y	z	U ₁₁	U ₂₂	U ₃₃	U ₁₂	U ₁₃	U ₂₃	U _{eq}
Cs	0.20052(2)	0.50015	0.50043(2)	0.0175(1)	0.0146(2)	0.0157(1)	0.0014(4)	0.00023(7)	0.00001(15)	0.01591(9)
Si	0.08469(9)	0.0004(7)	0.19052(7)	0.0056(3)	0.0034(3)	0.0052(3)	−0.0021(7)	−0.0005(2)	0.0018(8)	0.0047(2)
Al	0.41511(9)	−0.0036(7)	0.31650(7)	0.0047(3)	0.0023(4)	0.0053(3)	0.0006(7)	−0.0003(3)	−0.0008(8)	0.0041(2)
O1	0.0877(3)	−0.0047(24)	0.0104(2)	0.032(1)	0.013(1)	0.0035(8)	0.003(5)	0.0017(9)	0.001(2)	0.0161(7)
O2	0.0024(9)	−0.2413(14)	0.2502(3)	0.015(2)	0.012(2)	0.007(2)	−0.005(1)	−0.007(3)	0.003(2)	0.011(1)
O3	0.0040(9)	0.2404(14)	0.2551(3)	0.034(2)	0.013(2)	0.012(2)	−0.003(1)	0.008(3)	0.003(3)	0.020(1)
O4	0.2437(2)	0.0034(37)	0.2536(2)	0.010(1)	0.034(2)	0.028(1)	0.001(2)	−0.0056(9)	−0.009(2)	0.0241(9)
Cs	0.20402(5)	0.49994	0.50121(6)	0.0271(3)	0.0177(3)	0.0194(3)	0.0075(3)	−0.0001(2)	0.0023(4)	0.0214(2)
Si	0.08391(15)	0.01013(54)	0.19384(13)	0.0073(6)	0.029(1)	0.0086(5)	−0.0066(9)	−0.0005(5)	−0.0064(9)	0.0149(4)
Al	0.41630(17)	0.01126(58)	0.31297(14)	0.0080(7)	0.035(2)	0.0048(6)	−0.005(1)	−0.0015(5)	−0.006(1)	0.0159(5)
O1	0.0856(4)	0.0076(14)	0.0107(2)	0.032(2)	0.015(3)	0.005(1)	0.003(4)	0.004(2)	0.0001(2)	0.017(1)
O2	0.0359(5)	−0.2617(7)	0.2552(4)	0.039(3)	0.016(2)	0.012(2)	0.000(2)	0.008(2)	−0.003(2)	0.022(1)
O3	−0.0285(4)	0.2188(8)	0.2595(5)	0.037(3)	0.021(4)	0.014(2)	−0.003(2)	0.008(2)	0.003(2)	0.024(2)
O4	0.2432(3)	0.0817(11)	0.2531(4)	0.015(2)	0.054(4)	0.022(2)	0.007(2)	−0.008(1)	0.001(2)	0.030(2)

Notes: Estimated standard deviations appear in parentheses. The anisotropic displacement parameter exponent takes the form: $-2\pi^2[(ha^*)^2U_{11} + \dots + 2hka^*b^*U_{12}]$. U_{eq} is defined as one-third of the trace of the orthogonalized U_{ij} tensor.

are reported in Table 2. Bond distances and other geometrical parameters are listed in Table 3. Observed and calculated structure factors (for all the 3-individuals) are reported in Table 4¹

DISCUSSION AND CONCLUDING REMARKS

Like those of RbAlSiO₄ and TlAlSiO₄, the structure of the CsAlSiO₄ consists of two-dimensional tetrahedral sheets parallel to (001) in which the corner-sharing tetrahedra form an infinite mesh of six-membered rings (Fig. 3). Every tetrahedral sheet is connected to a sheet below and above which results in a three-dimensional tetrahedral framework (Figs. 3 and 4). Si-occupied and Al-occupied tetrahedra alternate along 6mRs, matching the 1:1 stoichiometry (Fig. 3). Apical O atoms of three neighboring tetrahedra in a ring point upward, whereas apical O atoms of the other three tetrahedra point down (Figs. 3 and 4). Neighboring pairs of sheets are held together by sharing triplets of apical O atoms in such a fashion that if there is an Al atom in the tetrahedron in the lower sheet, there is an Si atom in the tetrahedron above it and vice versa (Fig. 4). The general symmetry of CsAlSiO₄ (and RbAlSiO₄) is $Pc2_1/n$. The lowering of symmetry in TlAlSiO₄, from orthorhombic to monoclinic [$P2_1/n$ space group with $\gamma = 90.01(2)^\circ$], reported by Kyono et al. (2000) appears to be caused by the inert-pair effect of the Tl⁺ cation. However, the choice of the monoclinic space group seems to be poorly substantiated. The authors did not report a comparable refinement with orthorhombic symmetry and their tabulated observed-calculated structure factors are not available. This does not allow a further structural refinement with the orthorhombic $Pc2_1/n$ space group. In contrast, the disordered distribution of Al and Ti in the tetrahedral framework of CsAlTiO₄ implies the presence of only one independent tetrahedral site and a consequent increase of the general symmetry to $Imma$ (Gatehouse 1989).

Among the open-framework silicates containing 6mRs as a building block unit, a comparison can be drawn between the topology of the CsAlSiO₄ framework (i.e., ABW framework type) and that of tridymite, which represents the framework type of some important rock-forming feldspathoids such as nepheline and kalsilite. The differences between the framework configuration in tridymite and ABW type compounds are shown in Figure 5. In tridymite (or stuffed-tridymite structures), the orientation of tetrahedra belonging to the six-membered rings (...upward-downward-upward...) gives rise to a hexagonal $P6_3/mmc$ topo-

TABLE 3. Bond distances (Å) and angles (°) of (above) CsAlSiO₄ and (below) RbAlSiO₄

Cs-O1	3.646(3)	Si-O1	1.599(2)	Al-O1	1.721(2)
Cs-O1	3.393(11)	Si-O2	1.614(8)	Al-O2	1.749(8)
Cs-O1	3.350(11)	Si-O3	1.615(8)	Al-O3	1.743(8)
Cs-O2	3.222(6)	Si-O4	1.598(2)	Al-O4	1.708(3)
Cs-O2	3.205(6)				
Cs-O3	3.187(7)	O1-Si-O2	108.8(5)	O1-Al-O2	110.4(4)
Cs-O3	3.181(7)	O1-Si-O3	112.2(5)	O1-Al-O3	111.7(4)
Cs-O4	3.500(16)	O1-Si-O4	109.5(1)	O1-Al-O4	108.2(1)
Cs-O4	3.528(16)				
Cs-O4	3.552(15)	O2-Si-O3	108.4(4)	O2-Al-O3	107.5(4)
Cs-O4	3.579(15)	O2-Si-O4	110.0(7)	O2-Al-O4	108.4(7)
Cs-O2	3.835(15)				
Cs-O2	3.840(16)	O3-Si-O4	107.9(7)	O3-Al-O4	110.6(7)
Cs-O3	3.852(16)				
Cs-O3	3.874(16)	Si-O1-Al	177.7(5)		
		Si-O2-Al	141.1(2)		
		Si-O3-Al	137.8(2)		
		Si-O4-Al	177.6(1)		
Rb-O1	3.519(4)	Si-O1	1.598(2)	Al-O1	1.725(3)
Rb-O1	3.326(7)	Si-O2	1.605(5)	Al-O2	1.741(5)
Rb-O1	3.260(7)	Si-O3	1.623(5)	Al-O3	1.755(5)
Rb-O2	3.502(4)	Si-O4	1.602(4)	Al-O4	1.720(4)
Rb-O2	3.326(7)				
Rb-O2	2.935(4)	O1-Si-O2	109.2(3)	O1-Al-O2	110.9(3)
Rb-O3	3.551(4)	O1-Si-O3	111.4(3)	O1-Al-O3	110.7(3)
Rb-O3	3.358(4)	O1-Si-O4	108.4(2)	O1-Al-O4	107.2(2)
Rb-O3	2.886(4)				
Rb-O4	3.165(5)	O2-Si-O3	108.8(2)	O2-Al-O3	108.0(2)
Rb-O4	3.125(5)	O2-Si-O4	111.0(3)	O2-Al-O4	109.4(3)
Rb-O2	3.502(13)				
Rb-O3	3.551(14)	O3-Si-O4	108.0(3)	O3-Al-O4	110.7(3)
Rb-O3	4.033(17)				
Rb-O2	4.038(16)	Si-O1-Al	178.4(4)		
		Si-O2-Al	133.3(3)		
		Si-O3-Al	131.6(3)		
		Si-O4-Al	153.6(4)		

Note: Estimated standard deviations appear in parentheses.

logical symmetry (Fig. 5). In contrast, in Cs-,Rb-AlSiO₄, and other ABW type compounds, the aforementioned orientation of tetrahedra (upward-upward-upward-downward-downward-downward) gives rise to a reduction of the topological symmetry to $Imma$ (Fig. 4; Baur and Fischer 2000). The arrangement of pairs of tetrahedral sheets in (Cs,Rb)AlSiO₄ described above leaves void spaces between them that are larger than those in tridymite-type framework (i.e., 8mRs along [010] in (Cs-,Rb-) AlSiO₄ and 6mRs along [010] in stuffed-tridymite frameworks;

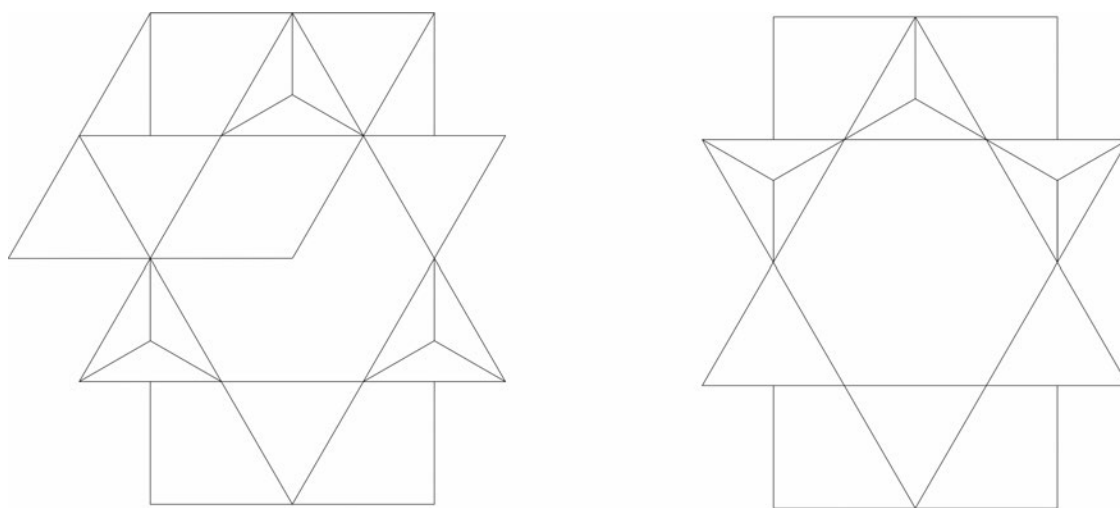


FIGURE 5. Idealized configuration of the tridymite-type framework, with a hexagonal $P6_3/mmc$ topological symmetry (left side) and that of the (Cs,Rb-)AlSiO₄ feldspathoid, characterized by the ABW-type $Imma$ topological symmetry (right side).

Gatta and Angel 2007). As a consequence, in stuffed-tridymite structures the extra-framework content is represented by K^+ , Na^+ , and Ca^{2+} sites (Palmer 1994, Gatta and Angel 2007 and references therein). In contrast, in the ABW framework type, large cations as Cs^+ , Rb^+ , Tl^+ , and Sr^{2+} (or smaller cations and water molecules, e.g., Li and nH_2O) can reside in the 8mR-channels (Baur and Fischer 2000 and references therein). However, a metastable polymorph of $KAlSiO_4$ (pseudo-orthorhombic with $a \sim 18.151$, $b \sim 10.551$, and $c \sim 8.490$ Å) has been prepared by K^+ ion exchange of orthorhombic $RbAlSiO_4$ by Minor et al. (1978).

The five quality structure refinements available for $CsAlSiO_4$ (Klaska 1977 and this study), $RbAlSiO_4$ (Klaska and Jarchow 1975 and this study) and $TlAlSiO_4$ (Kyono et al. 2000), respectively, allow some comparisons to be made. Tetrahedral bond lengths and the polyhedral volumes indicate a perfect fractionation of Al and Si in all structures (Table 3). However, the coordination polyhedron of the univalent cation is very irregular, as documented by the effective coordination number (ECoN, Table 5; Hoppe 1979) and the mean effective bond length (MEFBL, Table 3; Hoppe 1979, Rieder and Weiss 1998) for the cation itself and by the fictitious highest coordination point (*hcp*, Table 5; Rieder and Weiss 1998). The differences between *hcp* and the univalent atom are due to the fact that the cation lays off-center and the larger the departure the larger the corresponding decrease in ECoN and MEFBL. Surprisingly, Cs (the largest cation), known to accept a geometrically perfect 12-fold coordination in Cs-tetraferriannite (Mellini et al. 1996), is located asymmetrically in $CsAlSiO_4$ and its stagger can be seen well in projection onto the plane of the sixfold rings of tetrahedra (Fig. 3). Therefore, the nominal coordination of Cs in $CsAlSiO_4$ based on the ECoN calculation is at least 14-fold (Table 5). We can consider a bonding configuration of Cs represented by the nearest neighbor six O atoms in the ring below, six O atoms in the ring above, and three (apical, shared by both sheets) essentially in-plane with the cation (Fig. 6), with $CN(Cs) = 15$. A slightly different bonding environment is observed for Rb in $RbAlSiO_4$, where $ECoN(Rb) = 11-12$ (Table 5). In this case, it is reasonable

to consider four (or five) O atoms in the ring below, four (or five) in the ring above and three oxygen in-plane with the cation. If we calculate the mean effective bond length associated with the fictive highest coordination point and subtract from it the ionic radius, we obtain a difference that correlates with the stagger of the univalent cation (projected onto the plane of the 6mRs, Fig. 3). This may or may not indicate a causal relationship, but the correlation is worth mentioning (Fig. 7).

As shown in Table 3, the values of the co-respective $Cs-O_n$ and $Rb-O_n$ bond-distances and T-O-T angles in $CsAlSiO_4$ and $RbAlSiO_4$ are significantly different, giving rise to a different distortion of the 6mRs from the ideal hexagonal form (Fig. 3), due to the tetrahedral rotation (Table 5). The 6mR in the $CsAlSiO_4$ structure appears to be more regular than that in $RbAlSiO_4$, which in turn is more trigonally distorted (Fig. 3). More quantitatively, the “distortion parameter” of 6mR in $CsAlSiO_4$ [here defined as $\delta_{6mR} = (O2-O4)_{short}/(O2-O4)_{long}$; Fig. 3] is ~ 0.993 , whereas that of 6mR in $RbAlSiO_4$ is ~ 0.760 ($\delta_{6mR} = 1$ for an ideal hexagonal ring; the lower the δ_{6mR} -value, the higher the ring distortion from a regular hexagonal form). It appears, therefore, that the larger the ionic radius of the extra-framework cation, the lower the distortion of the 6mR/[001]. This is also supported by the comparative structural analysis among the ABW type compounds: the more di-trigonalized 6mR are observed for Li-bearing compounds (e.g., $LiAlSiO_4 \cdot H_2O$; Krogh Andersen and Ploug-Sørensen 1986; Baur and Fischer 2000). However, the ion size cannot be the only factor because the radii of Tl^+ and Rb^+ are quite close (Shannon 1976), yet the tetrahedral rotations, and the consequent 6mR distortion, are vastly different in $TlAlSiO_4$ and $RbAlSiO_4$, respectively (Table 5). We have also computed a correlation matrix involving 25 refined variables for $RbAlSiO_4$ and $TlAlSiO_4$. As can be expected, there is a significant positive correlation between the ionic radius of the extra-framework cation, its polyhedral volume, and the unit-cell volume. Also, as expected there are strong negative correlations between the tetrahedral rotation angles (Table 5) and unit-cell parameters perpendicular to the axis of rotation, a mechanism well known in sheet silicates. In

TABLE 5. Some characteristics of the isotypic TlAlSiO₄, RbAlSiO₄, and CsAlSiO₄ crystal structures

	TlAlSiO ₄ (Kyono et al. 2000)	RbAlSiO ₄ (Klaska and Jarchow 1975)	RbAlSiO ₄ (this study)	CsAlSiO ₄ (Klaska 1977)	CsAlSiO ₄ (this study)
Radius of the univalent cation (Å)	1.70	1.72	1.72	1.88	1.88
ECoN					
-univalent cation	6.22	8.34	8.37	11.02	11.58
-hcp	12.73	10.88	11.14	13.34	13.66
MEFBL (Å)					
-univalent cation	2.97	3.11	3.11	3.34	3.36
-hcp	3.27	3.19	3.20	3.39	3.40
Polyhedral volume (Å ³)					
-univalent cation (CN = 15)	89.45	90.01	89.63	95.67	95.11
-Al	2.66	2.69	2.68	2.68	2.66
-Si	2.14	2.17	2.13	2.13	2.13
θ, tetrahedral rotation angle (°)	0.8	28.0	26.0	6.2	0.2

Notes: Ionic radii are those for univalent cations in coordination XII (Shannon and Prewitt 1969; Shannon 1976). ECoN is the Effective Coordination Number of Hoppe (1979). MEFBL is a mean effective bond length weighted like MEFIR (Hoppe 1979), and hcp is the highest coordination point found by program MAPPER (Rieder and Weiss 1998). Polyhedral volumes were calculated with the program VOLCAL (Finger 1971). The tetrahedral rotation angle is defined as $\theta = [\sum_i (120 - \phi_i)]/6$, $i = 1, \dots, 6$, where ϕ_i represent the inner angles of the 6mR. In an ideal hexagonal ring, $\phi = 120^\circ$ and $\theta = 0^\circ$.

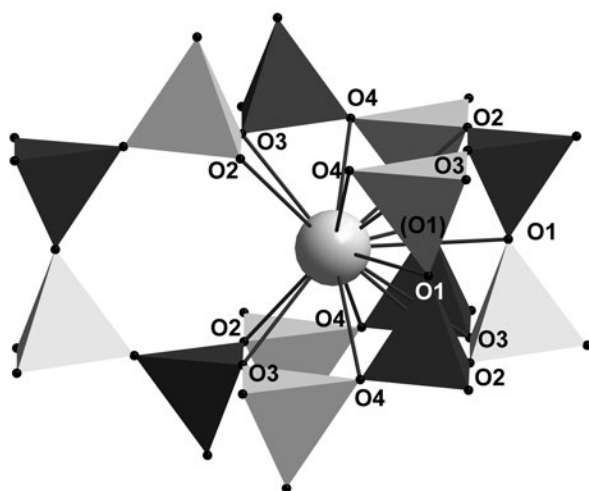


FIGURE 6. Configuration of the Cs-O (or Rb-O) bonding environment. The Cs-O (and Rb-O) bond-distance values are reported in Table 3. Dark-gray tetrahedra represent the Si-tetrahedra, whereas light-gray tetrahedra represent the Al-occupied ones.

the correlation matrix, the tetrahedral rotation does not correlate significantly with any other variable, so the effect of the lone pair of electrons, discussed by Kyono et al. (2000), may be the cause of the different tetrahedral rotation, and the 6mR distortion, in TlAlSiO₄ and RbAlSiO₄, respectively (Table 5).

The comparative crystal chemistry of the ABW type compounds shows that the flexibility of this framework type is high: the individual T-O/F-T angles scatter from 111 to 180° (Baur and Fischer 2000). The minimal free-diameter (i.e., the effective pore width, assuming an oxygen radius of 1.35 Å Baerlocher et al. 2001) of the 8mR in ABW type compounds are often <2 Å, smaller than those usually observed in zeolites. As a consequence, this class of materials does not exhibit typical zeolite-like properties (e.g., cation or molecular exchange capacity).

With respect to other Cs-aluminosilicates characterized by zeolite-like structures with large pores, such as Cs-4A zeolites (Vance and Seff 1975; Firor and Seff 1977) and Cs-bikitaite (CsAlSi₃O₁₂; Araki 1980), CsAlSiO₄ is more likely to retain Cs when immersed in a fluid phase, relative to the Cs-bearing zeolites (Klika et al. 2006). In addition, the topological configuration

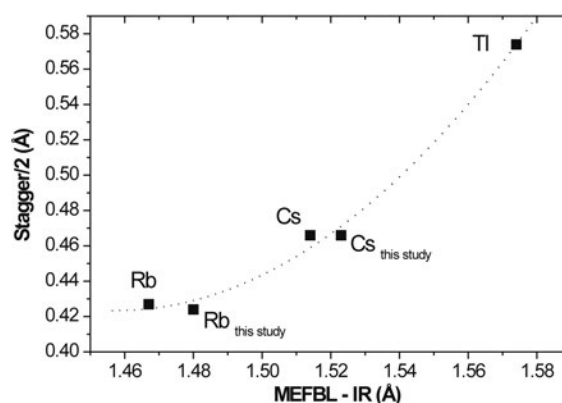


FIGURE 7. Half-stagger of univalent cations as a function of the ideal mean effective bond length (MEFBL) of the coordination polyhedron less the ionic radius (IR). Calculations are based on the data of Klaska and Jarchow (1975), Klaska (1977), Kyono et al. (2000), and the present results. The dotted line is provided as a visual guide.

of the Cs-polyhedron (and its bonding environment) and the small dimension of the pores implies better thermal and elastic stability of CsAlSiO₄ than those of the zeolitic Cs-aluminosilicates. In this light, CsAlSiO₄ can be considered as a functional material potentially usable for fixation and deposition of radioactive isotopes of Cs and can also be considered as a potential solid host for a ¹³⁷Cs γ -radiation source to be used in sterilization applications (Gallagher et al. 1977; Klaska 1977). A study on the thermo-elastic stability of CsAlSiO₄ is in progress.

ACKNOWLEDGMENTS

The authors are indebted with WH Baur, for a fruitful discussion on the structural features of compounds with ABW framework type, and M Nespolo, for the description of twinning in this class of compounds. The Associate Editor P Hoskin, the Technical Editor Andrew Locock, and the reviewers Th Armbruster and A Kyono are thanked for their useful suggestions.

REFERENCES CITED

- Araki, T (1980) Crystal structure of a cesium aluminosilicate, Cs(AlSi₃O₁₂) Zeitschrift für Kristallographie, 152, 207–213
- Baerlocher, Ch., Meier, W M., and Olson, D H (2001) Atlas of Zeolite Framework Types, 5th edition, 302 p Elsevier, Amsterdam
- Baur, W H. and Fischer, R X (2000) Zeolite-Type Crystal Structures and their Chemistry. Zeolite Structure Codes ABW to CZP. In W H Baur and R X Fischer, Eds., Landolt-Börnstein, Subvolume B, Numerical Data and Functional

- Relationships in Science and Technology, New Series, Group IV: Physical Chemistry Microporous and other Framework Materials with Zeolite-Type Structures, 14, p. 459 Springer-Verlag, Berlin
- Beger, R. M. (1969) Crystal structure and composition of pollucite *Zeitschrift für Kristallographie*, 129, 280–302
- Beswick, A. E. (1973) An experimental study of alkali metal distributions in feldspars and micas *Geochimica et Cosmochimica Acta*, 37, 183–208
- Comodi, P., Zanazzi, P. F., Weiss, Z., Rieder, M., and Drábek, M. (1999) Cs-tetraferri-annite: high-pressure and high-temperature behavior of a potential nuclear waste disposal phase *American Mineralogist*, 84, 325–332
- Drábek, M., Rieder, M., Viti, C., Weiss, Z., and Frýda, J. (1998) Hydrothermal synthesis of a Cs ferruginous trioctahedral mica *Canadian Mineralogist*, 36, 755–761
- Finger, L. W. (1971) VOLCAL, a program to calculate polyhedral volumes and distortion parameters Geophysical Laboratory, Carnegie Institution of Washington, Washington, D. C.
- Firor, R. L. and Seff, K. (1977) Zero-coordinate K Crystal structure of dehydrated cesium and potassium exchanged zeolite A, Cs,K₃-A *Journal of American Chemical Society*, 99, 6249–6253
- Gallagher, S. A., McCarthy, G. J., and Smith, D. K. (1977) Preparation and X-ray characterization of CsAlSiO₄ *Materials Research Bulletin*, 12, 1183–1190
- Gatehouse, B. M. (1989) Structure of CsAlTiO₄—a compound with TiO₄ tetrahedra *Acta Crystallographica*, C45, 1674–1677
- Gatta, G. D. and Angel, R. J. (2007) Elastic behavior and pressure-induced structural evolution of nepheline: Implications for the nature of the modulated superstructure *American Mineralogist*, 92, 1446–1455
- Hahn, T., Lohre, G., and Chung, S. J. (1969) A new tetrahedral framework structure in sulfates and fluoberyllates *Naturwissenschaften*, 56, 459
- Hawthorne, F. C., Cooper, M. A., Simmons, W. B., Falster, A. U., Laurs, B. M., Armbruster, T., Rossman, G. R., Peretti, A., Günter, D., and Grobety, B. (2004) Pezzottaite Cs(Be₂Li)Al₂Si₆O₁₈ A spectacular new beryl-group mineral from the Sakavalana pegmatite, Fianarantsoa province, Madagascar *Mineralogical Record*, 35, 369–378
- Hess, F. L. and Fahey, J. J. (1932) Cesium biotite from Custer County, South Dakota *American Mineralogist*, 17, 173–176
- Hoppe, R. (1979) Effective coordination numbers (ECoN) and mean fictive ionic radii (MEFIR)^[12] *Zeitschrift für Kristallographie*, 150, 23–52
- Kahlenberg, V., Fischer, R. X., and Baur, W. H. (2001) Symmetry and structural relationships among ABW-type materials *Zeitschrift für Kristallographie*, 216, 489–494
- Klaska, R. (1977) Hydrothermalsynthesen und Strukturuntersuchungen zu kation-enabhängigen Veränderungen von aufgefüllten Tetraedergerüsten aus dem Bereich der Feldspäte und seiner Vertreter Ph. D. dissertation, Universität Hamburg, Germany
- Klaska, R. and Jarchow, O. (1975) Die Kristallstruktur und die Verzwillingung von RbAlSiO₄ *Zeitschrift für Kristallographie*, 142, 225–238
- Klika, Z., Weiss, Z., Mellini, M., and Drábek, M. (2006) Water leaching of cesium from selected cesium mineral analogues *Applied Geochemistry*, 21, 405–418
- Krogh Andersen, E. and Ploug-Sørensen, G. (1986) The structure of zeolite Li-(ABW) determined from single crystal data *Zeitschrift für Kristallographie*, 176, 67–73
- Krogh Andersen, I. G., Krogh Andersen, E., Norby, P., Colella, C., and de'Gennaro, M. (1991) Synthesis and structure of an ABW type thallium aluminosilicate Zeolites, 11, 149–154
- Kyono, A., Kimata, M., and Shimizu, M. (2000) The crystal Structure of TlAlSiO₄: The role of inert pairs in exclusion of Tl from silicate minerals *American Mineralogist*, 85, 1287–1293
- Larson, A. C. and Von Dreele, R. B. (2000) GSAS—Generalized Crystal Structure Analysis System, Los Alamos National Laboratory, Report No. LA-UR-86-748
- Liebau, F. (1985) *Structural Chemistry of Silicates*, 347 p. Springer-Verlag, Berlin
- Mellini, M., Weiss, Z., Rieder, M., and Drábek, M. (1996) Cs-ferriannite as a possible host for waste cesium: Crystal structure and synthesis *European Journal of Mineralogy*, 8, 1265–1271
- Minor, D. B., Roth, R. S., Brower, W. S., and McDaniel, C. L. (1978) Alkali ion exchange reactions with RbAlSiO₄: A new metastable polymorph of KAlSiO₄ *Material Research Bulletin*, 13, 575–581
- Newnham, R. E. (1967) Crystal structure and optical properties of pollucite *American Mineralogist*, 52, 1515–1518
- Ni, Y. X. and Hughes, J. M. (1996) The crystal structure of nanpingite-2M₂, the Cs end-member of muscovite *American Mineralogist*, 81, 105–110
- Oxford Diffraction (2005) Oxford Diffraction Ltd., Xcalibur CCD system, CrysAlis Software system Oxfordshire, U. K.
- Palmer, D. C. (1994) Stuffed derivatives of the silica polymorphs In P. J. Heaney, C. T. Prewitt, and G. V. Gibbs, Eds., *Silica: Physical Behavior, Geochemistry and Materials Applications*, 29, p. 83–122. Reviews in Mineralogy, Mineralogical Society of America, Chantilly, Virginia
- Petříček, V. and Dušek, M. (2000) Jana2000 The crystallographic computing system Institute of Physics, Praha, Czech Republic
- Pitschke, W., Hermann, H., and Mattern, N. (1993) The influence of surface roughness on diffracted X-ray intensities in Bragg-Brentano geometry and its effect on the structure determination by means of Rietveld analysis *Powder Diffraction*, 8, 74–83
- Rieder, M. and Weiss, Z. (1998) MAPPER, a program for calculation of the mean effective bond length and locating the highest coordination point of polyhedra Institute of Materials Chemistry, VSB, Technical University of Ostrava, Czech Republic
- Shannon, R. D. (1976) Revised Effective Ionic Radii and Systematic Studies of Interatomic Distances in Halides and Chalcogenides *Acta Crystallographica*, A32, 751–767
- Shannon, R. D. and Prewitt, C. T. (1969) Effective ionic radii in oxides and fluorides *Acta Crystallographica*, B25, 925–946
- Vance, T. B. and Seff, K. (1975) Hydrated and dehydrated crystal structure of seven-twelfths cesium exchanged zeolites A *Journal of Physical Chemistry*, 79, 2163–2166

MANUSCRIPT RECEIVED JULY 3, 2007

MANUSCRIPT ACCEPTED JANUARY 15, 2008

MANUSCRIPT HANDLED BY PAUL HOSKIN